Inorganic Chemistry

Article

pubs.acs.org/IC

# Nanocage Structure Derived from Sulfonated β-Cyclodextrin Intercalated Layered Double Hydroxides and Selective Adsorption for Phenol Compounds

Xiangyu Xue,[†] Qingyang Gu,[†] Guohua Pan,[†] Jie Liang,[‡] Gailing Huang,[§] Genban Sun,[†] Shulan Ma,[†,*] and Xiaojing Yang[†]

[†]Beijing Key Laboratory of Energy Conversion and Storage Materials, College of Chemistry, Beijing Normal University, Beijing 100875, China

[‡]College of Hydropower and Information Engineering, Huazhong University of Science and Technology, Wuhan 430074, China

[§]School of Materials and Chemical Engineering, Zhengzhou University of Light Industry, Zhengzhou 450001, China

Supporting Information

**ABSTRACT:** Nanocage structures derived from decasulfonated β-cyclodextrin (SCD) intercalated ZnAl- and MgAl- layered double hydroxides (LDHs) were prepared through calcination-rehydration reactions. The ZnAl- and MgAl-LDH layers revealed different basal spacings (1.51 nm for SCD-ZnAl-LDH and 1.61 nm for SCD-MgAl-LDH) when contacting SCD, while producing similar monolayer and vertical SCD orientations with cavity axis perpendicular to the LDH layer. The structures of the SCD-LDH and carboxymethyl-β-cyclodextrin (CMCD)-LDH intercalates were fully analyzed and compared, and a structural model for the SCD-LDH was proposed. The thermal stability of SCD after intercalation was remarkably enhanced, with decomposition temperature increased by 230 °C. The adsorption property of the SCD-LDH composites for phenol compounds (the effects of adsorption time and phenol concentration on adsorption) was investigated completely. The monolayer arrangement of the interlayer SCD did not affect the adsorption efficiency toward organic compounds, which verified the highly swelling ability of the layered compounds in solvents. Both composites illustrated preferential adsorptive efficiency for 2,3-dimethylphenol (DMP) in comparison with other two phenols of hydroquinone (HQ) and tert-butyl-phenol (TBP), resulting from appropriate hydrophobicity and steric hindrance of DMP. For the two phenols of HQ and TBP, SCD-MgAl-LDH gave better adsorption capacity compared with SCD-ZnAl-LDH. The double-confinement effect due to the combination of the parent LDH host and intercalated secondary host may impose high selectivity for guests. This kind of nanocage structure may have potential applications as adsorbents, synergistic agents, and storage vessels for particular guests.

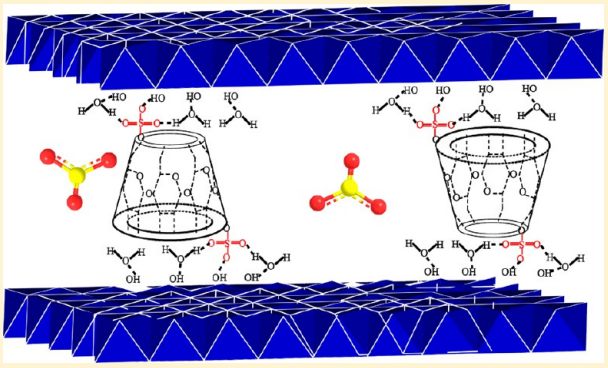

## INTRODUCTION

Host−guest hybrid materials can exhibit superior physicochemical characteristics and unique properties due to synergies of the host and guest components.[1] Inorganic host materials especially layered ion-exchangeable compounds offer a unique route to the design of the host−guest hybrids.[2] Layered double hydroxides (LDHs) are one kind of these inorganic host materials that have potential applications as catalysts,[3] ceramic precursors,[4] functional materials,[5] bioactive nanocomposites,[6] and adsorbents in separation science.[7]

Many organic hosts such as macrocyclic compounds including calixarenes, cyclodextrins and crown ethers are very famous because of their significant applications involving structural assembly[8] and molecule/ion recognition.[9] Cyclodextrins (CDs) and their derivatives have prospective applications in the food industry, pharmaceutical industry, agriculture, environmental protection, and other fields.[10] β-CD can increase the solubility of some pollutants, and catalyze their decomposition via the formation of inclusion compounds. Moreover, the hydrophobic environment and the cavity size have a significant impact for selective separation applications.[11] Before being used in separation technology, the water-soluble β-CD must be processed into a solid form, and the combination of β-CD with LDHs may achieve this goal.

Some anionic modified β-CD compounds have been combined with LDHs.[9c,12] Based on the recognition and inclusion properties of β-CD, the CD/LDH composites are expected to be potential sorbents for selective adsorption and separation of organic pollutants. There have been many reports involving in the intercalation of carboxymethyl-β-cyclodextrin (CMCD) into LDHs and the properties.[9c,11,12b,13] MgAl-LDH intercalated with CMCD cavities can selectively adsorb $I_2$,[14] and neutral guests as naphthalene,[15] anthracene,[16] ferrocene,[17]

Received: October 2, 2013
Published: January 14, 2014

   dx.doi.org/10.1021/ic402494m | Inorg. Chem. 2014, 53, 1521−1529

and many organic compounds.[12b] ZnAl-LDH intercalates with CMCD cavities were also used for selective adsorption of phenol and nitrobenzene,[11] racemic phenylalanine,[13b] dodecylbenzene,[18] and nucleosides adenosine and guanosine.[19]Table S1 in the Supporting Information lists the structural characteristic of some familiar CD-LDH intercalates and their related inclusion properties.

Sulfated cyclodextrins (SCD), on the other hand, have been widely used for enantiomeric separation, either by liquid chromatography using columns containing the materials bound to a solid support[20] or by capillary electrophoresis.[21] Sulfate ions could be grafted to the layers,[22] so after the intercalation, the leaching degree of SCD could be reduced. Additionally, the combination of high hydrophilic SCD with LDHs may produce different structure and adsorption behavior. However, there have been a lack of studies focusing on the SCD-LDHs preparation and their adsorption property, excluding the only case about intercalation of SCD(6) with a substitution degree of 6 into MgAl-LDH.[12a]

Nowadays, the widespread of organic contaminants in water is a main concern that impels researchers to look for remedies. Among the organic pollutants, phenol, pyridine, and nitrobenzene are very harmful to human health and the ecosystem,[23] and phenols are an important group, included as priority pollutants by USEPA (1980).[24] Activated carbon and zeolites were found to have relatively high adsorption capacity for phenols.[25,26] Magnetic porous carbon microspheres were also reported with adsorption properties for phenol and nitrobenzene.[27] LDH materials may be attractive as filters for the contaminants. The CMCD-ZnAl-LDH intercalates have demonstrated preferential adsorption for phenol over nitrobenzene.[12] However, the selective adsorption of phenol compounds is rarely reported. Herein, we investigate the intercalation of SCD(10) with a substitution degree of 10 into the MgAl- and ZnAl-LDHs by calcination−rehydration reaction. The composites revealed high adsorption capacity and obvious selectivity toward three phenolic compounds, hydroquinone (HQ), 2,3-dimethylphenol (DMP) and tert-butylphenol (TBP). These composites may become promising materials because of the synergy of the hydrophilic parent LDH host and the nanocages of the intercalated secondary macrocyclic host.

## EXPERIMENTAL SECTION

**Reagents.** $\beta$-CD was purchased from Aldrich. Other chemicals including concentrated sulfuric acid, $ZnCl_2$, $AlCl_3{\cdot}6H_2O$, $Al(NO_3)_3{\cdot}9H_2O$, $Mg(NO_3)_2{\cdot}6H_2O$, urea, hexamethylenetetramine (HMT), ethanol, HQ, DMP, and TBP were of analytical grade and used without further purification.

**Synthesis of SCD Intercalated LDHs.** SCD(10) was synthesized according to the procedure described in the literature using 90% $H_2SO_4$.[28] The average substitution number 10 of sulfonic acid groups per $\beta$-CD molecule was determined by ICP and elemental analysis.

MgAl-$CO_3$-LDH (Mg/Al molar ratio is 2:1) was prepared by a precipitation method similar to the literature,[29] using HMT hydrolysis at 140 °C. ZnAl-$CO_3$-LDH (Zn/Al molar ratio is 2:1) was synthesized by a reflux method reported previously.[30] The as-prepared MgAl- and ZnAl-LDHs were calcined at 500 °C for 2 h to produce the layered double oxide (LDO) samples.

Subsequently, the as-prepared composites of SCD-LDHs were prepared by a calcination-rehydration method. Typically, each SCD solution (20 mL) with a various concentration was placed in a 50 mL Erlenmeyer flask together with the LDO precursor (0.1 g) and the mixture was stirred for 48 h in a water bath set at 25 °C under a $N_2$ atmosphere. The resulting precipitates were washed with distilled water and dried under a vacuum at 40 °C for 24 h. The intercalated amount of SCD was measured using CHN and ICP analyzer.

**Adsorption Experiments.** A batch method was used to carry out the adsorption experiments. The effects of adsorption time and phenol concentration under the neutral conditions were investigated. All reported experiment data are the averages of duplicate determinations.

**Effect of Adsorption Time.** A series of 5 mL aqueous solutions of phenols (concentration: 0.5 mg/ml; pH ∼7) were added to centrifuge tubes and 0.03 g SCD-LDH composite was dispersed thoroughly in the solution. Then the centrifuge tubes were placed in a test tube rack at room temperature for a series of time (2, 4, 6, and 8 days) and gently shaken for several times per day. After the adsorption, the solution and the solid sample were separated by centrifugation. The solids were taken to do XRD and IR measurements.

**Effects of Phenol Concentration.** The SCD-LDH composites were dispersed in solutions with different phenol concentrations, and the mixture solutions were placed in oscillator at room temperature and shaken at 200 r/m for 48 h.

For quantitative analysis, standard calibration curves of phenols, with concentrations of 0.01, 0.02, 0.03, 0.04, and 0.05 mg/mL of the standard solutions, were obtained by means of an UV−vis spectrophotometer by monitoring the absorbance of standard solutions at their wavelengths of maximum absorption. The adsorption capacity for phenols adsorbed by the SCD-LDH composite ($q_e$, mg/g) was calculated by the difference between the initial concentration ($C_0$) and equilibrium concentration ($C_e$) per gram of LDH adsorbent,[19] and the adsorption rate of phenols ($\omega$%) was calculated as the adsorbed phenols (difference between $C_0$ and $C_e$) divided by the initial phenol amount.

$$q_e = (C_0 - C_e)V_s/m_{LDH} \quad (1)$$

$$\omega\% = (C_0 - C_e)V_s/m_{ph}100 \quad (2)$$

where $C_0$ (mg/ml) and $C_e$ (mg/ml) are the initial and equilibrium concentrations of phenols, respectively. $V_s$ is the solution volume (mL), $m_{LDH}$ is the mass of LDH adsorbent (g), and $m_{ph}$ is the mass of phenol (g).

All of the above syntheses, experiments and adsorption operations underwent several repetitions and the obtained results have good reproducibility.

**Characterization Techniques.** Powder X-ray diffraction (XRD) data of the samples were recorded with a Shimadzu XRD-6000 diffractometer, using Cu K$\alpha$ radiation between 4.5 to 70° with a scanning rate of 10°/min$^{-1}$. FT-IR spectra were obtained with a Vector 22 (Bruker) spectrophotometer in the range of 4000−400 cm$^{-1}$ using KBr disk method. CHN data were obtained with an Elementar vario elemental analysis instrument. Metal ion analysis was performed by inductively coupled plasma (ICP) emission spectroscopy with a Shimadzu ICPS-7500 instrument. The UV−vis absorption spectrophotometer (Shimadzu UV-2501PC) was employed to measure the absorption spectra of aromatic compounds in the 200−400 nm wavelength range. The concentrations of phenols (HQ, DMP and TBP) in the solutions, before and after the adsorption, were determined by UV−vis absorption spectroscopy at the wavelength of 312, 293, and 296 nm, respectively.

## RESULTS AND DISCUSSION

**Structures of LDHs and Composite SCD-LDHs.** The XRD patterns of $CO_3$-LDH, calcined products LDO, and the restored composites SCD-LDHs are displayed in Figure 1. The basal spacing ($d_{basal}$) is estimated using the ($d_{003}$ + 2$d_{006}$ + 3$d_{009}$)/3. From patterns a and b in Figure 1, the basal spacing of 0.76 nm is characteristics of a $CO_3$-LDH phase.[12c] After calcination, the disappearance of the series of (00$l$) reflections and appearance of peaks at the 2$\theta$ range of ∼30−50° (Figure 1c, d) indicated the destruction of the LDH layers and the formation of LDO. When the SCD solution was contacted with LDO, the restoration of the lamellar structure and the entrance


dx.doi.org/10.1021/ic402494m | Inorg. Chem. 2014, 53, 1521−1529

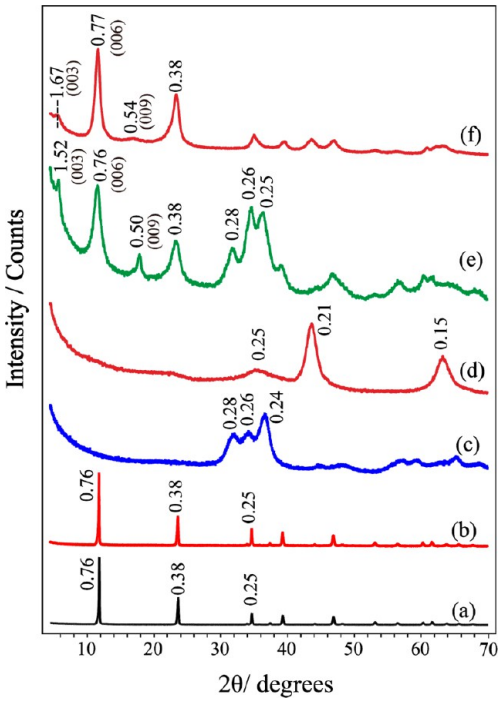


**Figure 1.** XRD patterns of precursors (a) ZnAl-$CO_3$-LDH and (b) MgAl-$CO_3$-LDH, calcined products (c) ZnAl-LDO and (d) MgAl-LDO, (e) composites SCD-ZnAl-LDH and (f) SCD-MgAl-LDH, respectively. The *d*-values are given in nanometers.

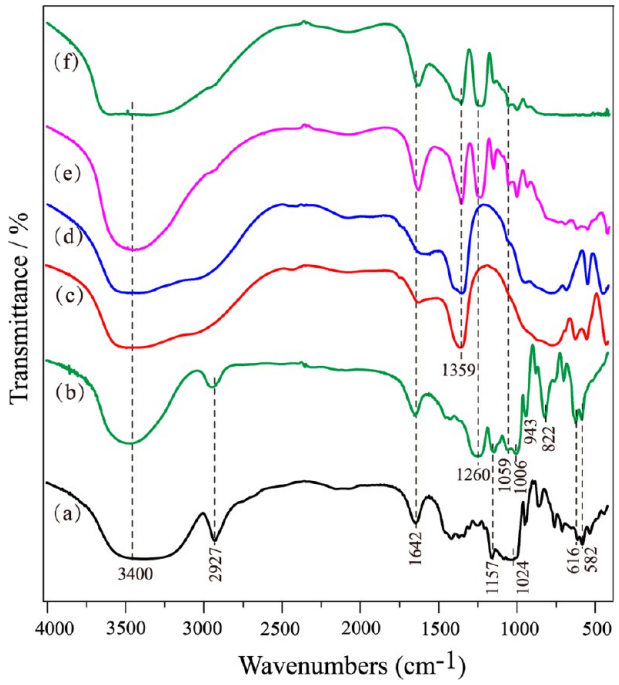


**Figure 2.** FT-IR spectra of (a) *β*-CD, (b) SCD, (c) ZnAl-$CO_3$-LDH (d), MgAl-$CO_3$-LDH, and composites (e) SCD-ZnAl-LDH, (f) SCD-MgAl-LDH, respectively.

of SCD into the interlayer space were verified, as shown in patterns e and f in Figure 1. New series of (00*l*) reflections being characteristics of layered compounds appeared, and from $(d_{003} + 2d_{006} + 3d_{009})/3$, increased $d_{basal}$ of 1.51 nm for composite SCD-ZnAl-LDH and 1.61 nm for SCD-MgAl-LDH were obtained. Compared with the only case for SCD(6) intercalated MgAl-LDH with a $d_{basal}$ of 1.58 nm,[12a] the present SCD(10)-MgAl-LDH gave a slightly larger $d_{basal}$ (1.61 nm). This may be due to the larger torus thickness of the present SCD with a substitution degree of 10, for which both of the two faces of the CD molecules were attached by sulfonic groups. Additionally, strong peaks at 0.76/0.77 nm were observed, which might result from the existence of $CO_3$-LDH phase. The presence of $CO_3$-LDH is corroborated by the FT-IR spectra with the expected $\nu_3$ mode of the carbonate species at 1359 $cm^{-1}$ (Figure 2). This indicates that the intercalation products are mixed phases. The overlap of the (006) reflection of the composites and the (003) deflection of $CO_3$-LDH phase may account for the enhanced intensity of this peak.

The two composites of SCD-ZnAl-LDH and SCD-MgAl-LDH have the same interlayer guest but different LDH layers, thus their different $d_{basal}$ values may come from varied combination interactions between the SCD guest with the layer. The 1.51 nm $d_{basal}$ of SCD-ZnAl-LDH in the present case is the same as that found for CMCD-ZnAl-LDH.[11,31] It is found for the intercalation of CMCD (with a substitution degree of 3.8 or 4.1) into LDHs, the ZnAl system normally gave a $d_{basal}$ of 1.52−1.64 nm,[11,13d,18,31] whereas the MgAl system usually produced much larger $d_{basal}$ of 2.45/2.46 nm, as shown in Table S1 in the Supporting Information. This also showed a much obvious difference of the nature for the two LDH layers.

The structure of cyclodextrin should be regarded as truncated cone rather than a cylinder.[10a] There are seven primary and 14 secondary hydroxyl groups along the *β*-cyclodextrin cavity, in which the primary hydroxyl groups located on the narrow side of the cyclodextrin ring are more readily substituted than the secondary hydroxyl groups. For SCD(10), the seven primary hydroxyl groups on the narrow side should be completely substituted by sulfate groups, and on the wide side, there will be three sulfate groups due to the substitution. *β*-CD has an approximate torus thickness of 0.78 nm, an outer diameter of 1.53 nm and an inner diameter of 0.78 nm.[9c,10a,12a] On the basis of the LDH layer height of 0.48 nm,[32] the $d_{basal}$ of 1.51 and 1.61 nm corresponded to gallery distances of 1.03 nm (= 1.51−0.48) for SCD-ZnAl-LDH and 1.13 nm (= 1.61−0.48) for SCD-MgAl-LDH. Taking into account the dimensions of 1.53 × 0.78 × 0.78 $nm^3$ for *β*-CD, the interlayer SCD would adopt a monolayer vertical arrangement with their cavity axis perpendicular to the LDH layer, because the 1.03 and 1.13 nm gallery distances are much smaller than the double of the torus thickness (0.78 × 2 = 1.56 nm) and its one outer diameter (1.53 nm). The proposed arrangement of SCD anions in the interlayer was shown in Scheme 1. The monolayer vertical arrangement of SCD molecules in the present case is similar to that reported for nearly all CMCD intercalated ZnAl-LDH.[11,13d,18,31] Whereas, for MgAl-LDH system with CMCD intercalation, the bilayer arrangement of CMCD was usually found.[13c,14−17] We can see for the same CMCD guest, the ZnAl-LDH layer prefers a monolayer arrangement while MgAl-LDH layer favors a bilayer one, which reveals the large difference of the two kinds of layers. In the present case, the SCD guest in MgAl-LDH system adopted a monolayer arrangement, possibly because of the larger negative charge on both sides of the CD molecule.

The area per unit charge ($S_{charge}$) is usually used to explain the intercalation structure. When the $S_{charge}$ of the intercalated species is smaller than that of the LDH layer, then a monolayer orientation will be formed, and when the former is bigger than


dx.doi.org/10.1021/ic402494m | Inorg. Chem. 2014, 53, 1521−1529

Scheme 1. Arrangement of SCD Anions in the Interlayer of LDH

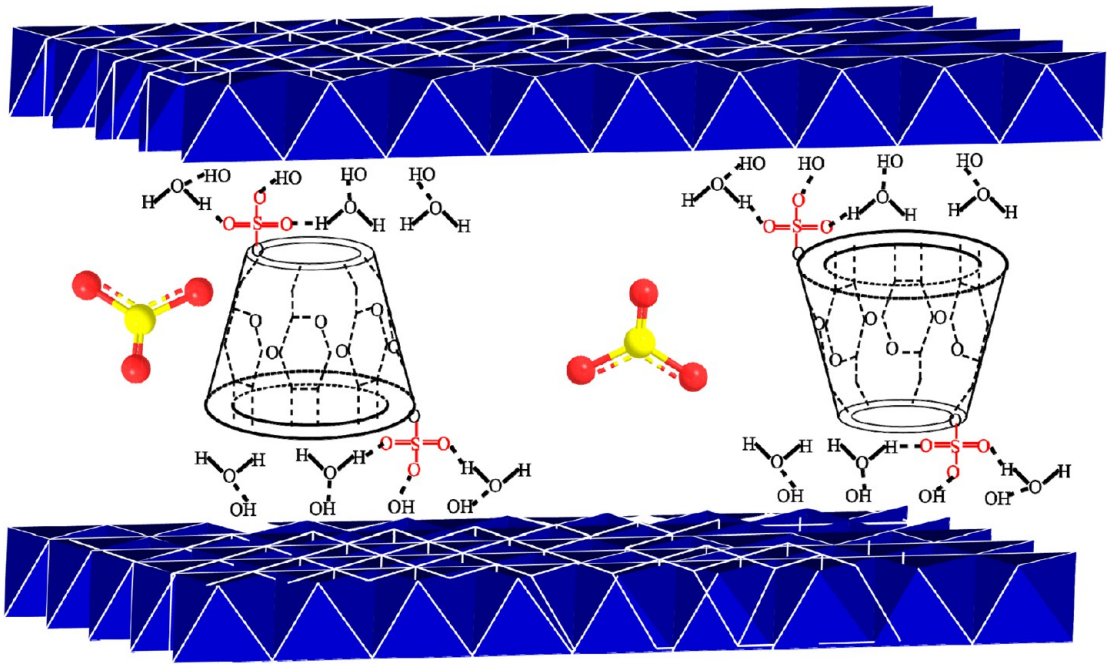

the latter, then a bilayered fashion will exist.[33] Calculated from the outer diameter of 1.53 nm (D) of $\beta$-CD with −10 valence, its $S_{charge}$ value is $(D^2\pi/4)/10 = 0.18$ nm$^2$, being smaller than the $S_{charge}$ value of LDH layer (0.24 nm$^2$),[34] so a monolayer arrangement is reasonable.[33] In addition, $CO_3^{2-}$ anions as well as water molecules are allowed to enter into the free space in the interlayer gallery.

Through analyzing the CMCD intercalated LDHs, we know the ZnAl system normally gave a smaller $d_{basal}$ (1.52−1.64 nm) and monolayer fashion of CMCD,[11,13d,18,31] while the MgAl system usually had much larger $d_{basal}$ (2.46 nm) and bilayer arrangement.[13c,14−17] In the present case, the tight combination motif of the SCD anions with the two kinds of LDH layers should result from the stronger electrostatic interaction because of the larger negative charge (10) of SCD. In the intercalation of natural (nonanionic) CD into MgAl-LDH, bilayer arrangement of CD was also found,[12c] showing the MgAl layer prefers a bigger gallery space.

**FT-IR Spectra, Morphology, And Thermal Analysis.** Figure 2 shows the IR spectra of $\beta$-CD, SCD, $CO_3$-LDH, and composites SCD-LDHs. The broad absorption bands at 3400 and 1642 cm$^{-1}$ correspond to the stretching vibration of the hydroxyl group in the LDH layers, interlayer water and physically adsorbed water molecules. For $\beta$-CD (Figure 2a) and SCD (Figure 2b), the absorption band at 2927 cm$^{-1}$ is due to the stretching vibration of $-CH_2$ of CD skeleton, and those at 1157, 1024, and 943 cm$^{-1}$ can be assigned to the vibrations of $\delta_{C-O}$ and $\nu_{C-O}$ of glucose units.[12a,35] Compared with $\beta$-CD, the spectra of SCD (Figure 2b) shows characteristic absorptions of $-SO_3$ group appearing at 1260 ($\nu_{SO2}$) and 1059 cm$^{-1}$ ($\nu_{C-O-S}$).[12a,36] The band at 1359 cm$^{-1}$ in $CO_3$-LDH precursors (Figure 2c,d) is from the $CO_3^{2-}$. In the SCD-LDH composites (Figure 2e, f), characteristic bands for $-SO_3$ group of SCD at 1260 and 1059 cm$^{-1}$ were also observed, which provided further evidence for the introduction of SCD into the LDHs. The band at 1359 cm$^{-1}$ in the composites indicates $CO_3^{2-}$ coexisted with SCD anions in the interlayer, in well agreement with the XRD results and elemental analysis data that will be discussed later.

Figure 3 showed the SEM images of the staring material of MgAl-$CO_3$-LDH, the composites SCD-MgAl-LDH and SCD-ZnAl-LDH, and the product after SCD-ZnAl-LDH adsorbed HQ. The MgAl-$CO_3$-LDH (Figure 3a.a′) had a very good hexagonal prismatic shape, whereas after the calcination−rehydration reaction, the composite SCD-LDH (Figure 3b, b′, c, c′) retained the hexagonal morphology but with small pores and coarse surface. Regardless, the layered structural characteristic is evident. The adsorption process did not change the hexagonal prismatic shape of the SCD-LDH composite (Figure 3d, d′), which indicates considerable stability of the composite samples in the phenolic solutions.

The TG-DTA curves of SCD, MgAl-$CO_3$-LDH and composite SCD-MgAl-LDH were shown in Figure 4. The SCD precursor (Figure 4a) exhibits three weight loss events. The first event (50−200 °C) is attributed to the loss of adsorbed and cavity water;[9c] the second sharp event (200−270 °C) is due to the decomposition and partial combustion of SCD, accompanying by an exothermic peak at 250 °C and endothermic peak at 260 °C in the DTA curve; the third weight loss (270−430 °C) is the result of combustion of SCD, with a corresponding strong exothermic peak at 420 °C in the DTA curve (Figure 4a′). For comparison, we showed the TG-DTA curves of MgAl-$CO_3$-LDH precursor. It exhibits three weight loss stages. The first (120−240 °C) and second (240−340 °C) correspond to the removal of water (from both the internal gallery surface and the external surfaces); the third (340−540 °C) is due to dehydroxylation of the brucite-like layers as well as decomposition of the $CO_3^{2-}$ anions. The DTA curve shows three endothermic peaks (Figure 4b′) at 235, 317, and 440 °C, respectively. For the SCD-MgAl-LDH composite, two obvious steps (Figure 4c) are found: the first (50−600 °C) step is due to loss of both adsorbed water and SCD cavity water molecules, the dehydroxylation of the LDH layer, the decomposition of the SCD anions, with a corresponding exothermic peak at 230 °C in the DTA curve (Figure 4c′); the second step (600−750


dx.doi.org/10.1021/ic402494m | Inorg. Chem. 2014, 53, 1521−1529

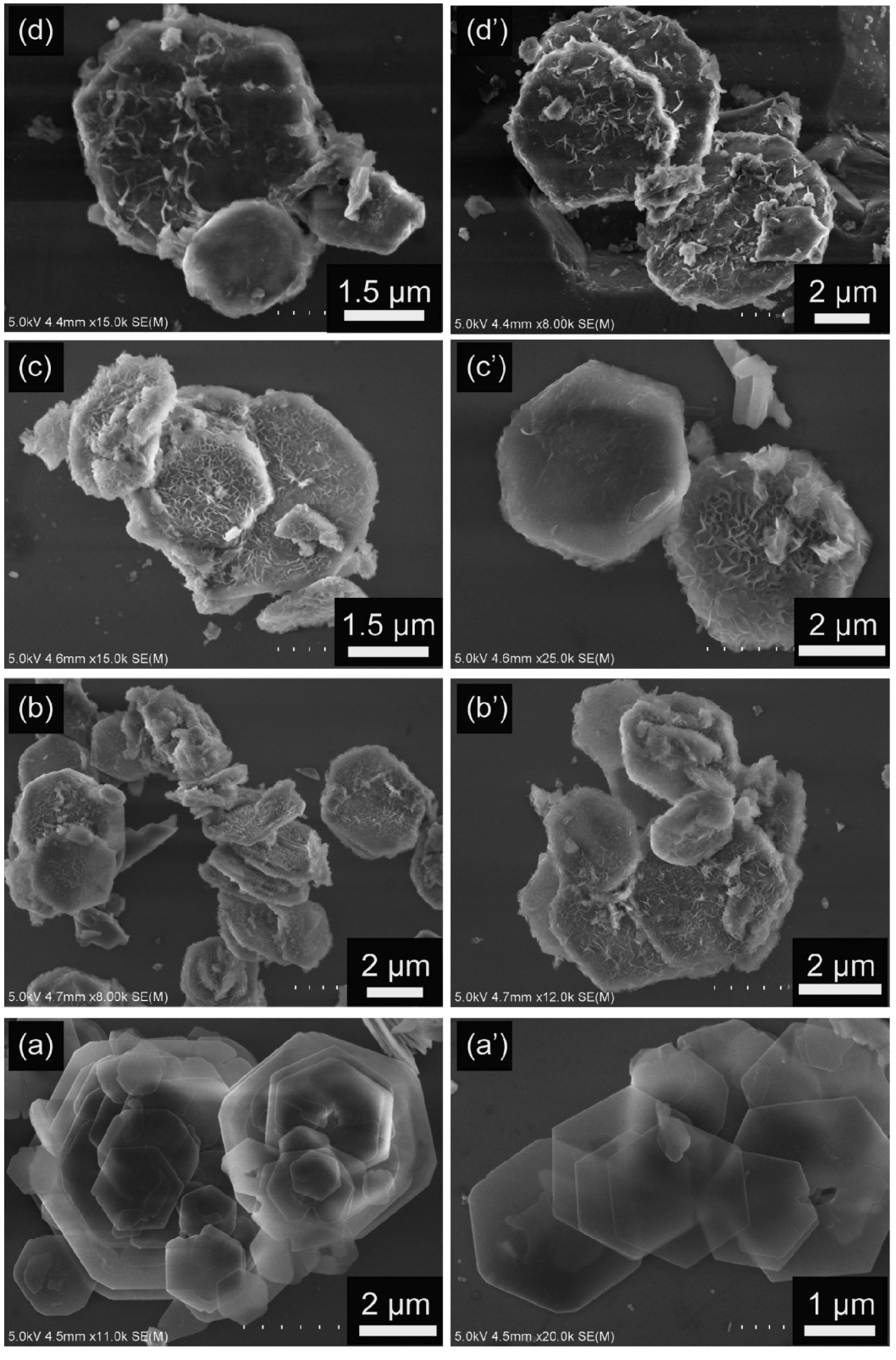


**Figure 3.** SEM images of (a, a′) MgAl-$CO_3$-LDH, (b, b′) SCD-MgAl-LDH, (c, c′) SCD-ZnAl-LDH, and (d, d′) after SCD-ZnAl-LDH adsorbed HQ, respectively.

°C) can be attributed to the combustion of interlayer SCD, with a corresponding exothermic peak at 650 °C in the DTA (Figure 4c′). Compared to pure SCD salt (Figure 4a′), the combustion temperature of interlayer SCD anion in the composite is increased by some 230 °C (650 − 420 = 230) through intercalation. This significant increase in thermal stability of SCD may indicate that the diffusion of oxygen is restricted by the presence of the host layers.[12a]

**Chemical Compositions of SCD and Composites.** On the basis of the CHN and ICP analyses, the chemical formula of


dx.doi.org/10.1021/ic402494m | *Inorg. Chem.* 2014, 53, 1521−1529

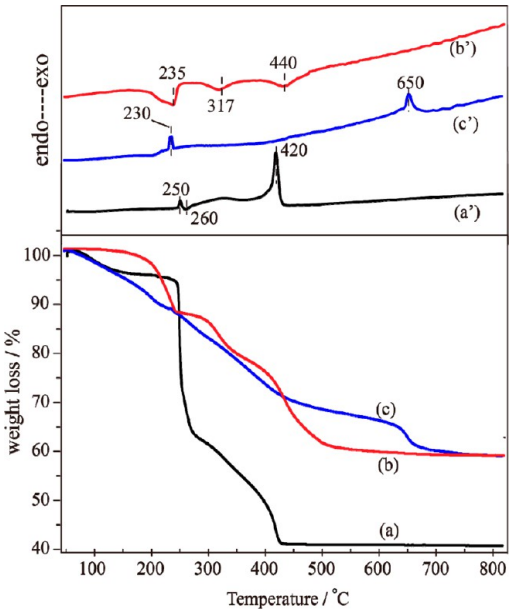


**Figure 4.** TG-DTA curves of (a, a′) SCD, (b, b′) MgAl-$CO_3$-LDH, and (c, c′) the composite SCD-MgAl-LDH, respectively.

SCD (in the form of a sodium salt) is described as $C_{42}H_{60}O_{35}(SO_3Na)_{10}\cdot 14H_2O$. This revealed a substitution degree of 10. The formula of the two composites SCD-ZnAl-LDH and SCD-MgAl-LDH were determined to be $Zn_{0.68}Al_{0.32}(OH)_2\cdot(SCD)_{0.008}(CO_3)_{0.081}(OH)_{0.075}$ and $Mg_{0.68}Al_{0.32}(OH)_2\cdot(SCD)_{0.011}(CO_3)_{0.004}(OH)_{0.20}\cdot 0.4H_2O$, respectively. The ICP and CHN analysis results and chemical formula of SCD and composites were shown in Table 1. From charge balance and the compositions, we can see in the two composites, the charge of SCD is around −10, corresponding to the substitution degree of 10. From the compositions, the hydroxyl ions were also cointercalated in the interlayer space, which was also found in the previous report.[12c]

**Adsorption Behavior of SCD-LDH Composites.** The adsorption behavior of the composites SCD−LDHs toward phenols was investigated by UV−vis spectrophotometry. Figure S1 in the Supporting Information shows the UV−vis spectra of the standard aqueous solutions of phenols (HQ, DMP, and TBP). The spectra of the standard aqueous solutions of phenols show a broad absorption band. Based on the concentrations of phenols and the absorbance at the wavelength of maximum absorption of their spectra, the standard curve equations are obtained as shown below. The standard curve equations are used to estimate the concentration of phenols before and after adsorption.

$$\text{HQ: Abs} = 32.36c + 0.1478R^2 = 0.9881 \quad (3)$$

$$\text{DMP: Abs} = 164.56c + 0.0195R^2 = 0.9962 \quad (4)$$

$$\text{TBP: Abs} = 10.44c + 0.046R^2 = 0.991 \quad (5)$$

**Effect of Adsorption Time on the Adsorption Behavior.** First the study of the effect of different adsorption time (2, 4, 6, and 8 days) on the adsorption behavior was carried out. Table 2 displays the adsorption results of SCD-ZnAl-LDH composite for HQ and DMP, with the same initial phenol concentration of 0.5 mg/mL. It can be observed that the adsorption capacity and adsorption rate for HQ nearly remain unchanged from 2 to 6 days ($\omega \approx 62\%$) but decreases within 8 days ($\omega \approx 46\%$), which suggests too long of a time may cause the release of the adsorbed phenols. However, the adsorption capacity of DMP slightly increases with the adsorption time ($\omega$ = 90−93%). Here the phenols of HQ and DMP exist as neutral molecular form at pH 6−8, therefore, the difference of the adsorption capacity may be due to the hydrophobic nature of the two phenols. The DMP molecules with two methyl groups should have higher hydrophobic nature than HQ with only two hydroxyl groups. This might result in a stronger recognition (inclusion) interaction of the SCD cavity for the phenols. The results are similar to those found for the inclusion of benzene derivatives into $\beta$-CD cavity.[37] The selective adsorption of phenols can be achieved well in 2 days. Therefore, the adsorption time of 2 days (48 h) was selected to carry out the subsequent experiments.

**Effect of Phenol Concentration on Adsorption Behavior.** The SCD-LDH composites were dispersed into the phenol solutions (neutral condition) with different concentrations and then shaken for 48 h at room temperature. The adsorption capacities of SCD-ZnAl-LDH and SCD-MgAl-LDH toward different concentrations of phenols within 48 h contact time are shown in Tables 3 and 4, respectively. It was found that the adsorption amount of the SCD-LDH composite for the three phenols increased clearly with the increase in starting concentration; however, the adsorption rate for HQ and TBP decreases with the increase in the concentration, whereas for DMP, the adsorption rate basically remains unchanged. As shown in Table 3, the adsorption rates of SCD-ZnAl-LDH are from 95 to 70% for HQ ($C$ = 0.1−0.5 mg/mL), from 88 to 65% for TBP ($C_0$ = 0.36−1.80 mg/mL), and retain ∼95% for DMP ($C_0$ = 0.1−0.5 mg/mL). For SCD-MgAl-LDH (Table 4), the adsorption rates are from 98% to 31% for HQ ($C_0$ = 0.4−2.0 mg/mL), from 95 to 67% for TBP ($C_0$ = 0.36−1.80 mg/mL), and keep ∼95% for DMP ($C_0$ = 0.4−2.0 mg/mL). Additionally, we can see different adsorption behavior of the two composites: SCD-ZnAl-LDH (Table 3) achieved the largest adsorption rates of 95% for HQ ($C_0$ = 0.1 mg/mL), 95% for DMP ($C_0$ = 0.1 mg/mL), and 88% for TBP ($C_0$ = 0.36 mg/mL), at the same time, SCD-MgAl-LDH (Table 4) got the largest adsorption rates of 98% for HQ ($C_0$ = 0.4 mg/mL), 95%

**Table 1. ICP and CHN Analysis Results and Chemical Formula of SCD and Composites**

| | content, found (calcd) (wt %) | | | | | | |
|---|---|---|---|---|---|---|---|
| sample | Mg | Zn | Al | C (%) | H (%) | Na (%) | chemical formula |
| SCD | | | | 20.75 | 3.61 | 9.92 | $C_{42}H_{60}O_{35}(SO_3Na)_{10}\cdot 14H_2O$ |
| | | | | (20.95) | (3.66) | (9.56) | |
| SCD-ZnAl-LDH | | 50.03 | 9.87 | 5.52 | 2.88 | | $Zn_{0.68}Al_{0.32}(OH)_2\cdot(SCD)_{0.008}$ |
| | | (50.08) | (9.67) | (5.68) | (2.90) | | $(CO_3)_{0.081}(OH)_{0.075}$ |
| SCD-MgAl-LDH | 18.05 | | 9.45 | 6.07 | 4.02 | | $Mg_{0.68}Al_{0.32}(OH)_2\cdot(SCD)_{0.011}$ |
| | (18.08) | | (9.43) | (6.12) | (3.80) | | $(CO_3)_{0.004}(OH)_{0.20}\cdot 0.4H_2O$ |


dx.doi.org/10.1021/ic402494m | Inorg. Chem. 2014, 53, 1521−1529

Table 2. Adsorption Capacity of SCD-ZnAl LDH for HQ and DMP at Varied Adsorption Times[a]

| | | before adsorption | | after adsorption | | | |
|---|---|---|---|---|---|---|---|
| | time (days) | $C_0$ (mg/mL) | pH | $C_e$ (mg/mL) | pH | adsorption capacity, $q_e$ (mg/g) | adsorption rate, $\omega$ (%) |
| HQ | 2 | 0.5 | 6.63 | 0.19 | 6.71 | 51.62 | 62.15 |
| | 4 | 0.5 | | 0.19 | 6.49 | 52.24 | 62.89 |
| | 6 | 0.5 | | 0.19 | 6.81 | 51.59 | 61.90 |
| | 8 | 0.5 | | 0.27 | 6.96 | 38.43 | 46.58 |
| DMP | 2 | 0.5 | 6.96 | 0.0398 | 7.34 | 59.83 | 90.13 |
| | 4 | 0.5 | | 0.0396 | 7.32 | 59.68 | 90.18 |
| | 6 | 0.5 | | 0.0311 | 7.31 | 60.08 | 92.29 |
| | 8 | 0.5 | | 0.0292 | 7.21 | 62.00 | 92.76 |

[a]Two repeating adsorption operations were done to evaluate these results.

Table 3. Adsorption Capacity of SCD-ZnAl-LDH for HQ, DMP and TBP at Different Concentrations[a]

| | concentration, $c$ (mg/mL) | | | |
|---|---|---|---|---|
| | before adsorption $C_0$ | after adsorption $C_e$ | adsorption capacity, $q_e$ (mg/g) | adsorption rate, $\omega$ (%) |
| HQ | 0.1 | 0.0047 | 11.79 | 95.30 |
| | 0.2 | 0.0328 | 21.00 | 83.60 |
| | 0.3 | 0.060 | 30.00 | 80.00 |
| | 0.4 | 0.103 | 36.81 | 74.18 |
| | 0.5 | 0.149 | 43.62 | 70.14 |
| DMP | 0.1 | 0.0049 | 11.80 | 95.10 |
| | 0.2 | 0.0083 | 23.84 | 95.85 |
| | 0.3 | 0.0092 | 36.26 | 96.93 |
| | 0.4 | 0.018 | 47.27 | 95.50 |
| | 0.5 | 0.025 | 58.84 | 95.08 |
| TBP | 0.3582 | 0.0435 | 31.41 | 87.86 |
| | 0.7165 | 0.1226 | 59.27 | 82.89 |
| | 1.0747 | 0.2184 | 85.63 | 79.68 |
| | 1.4330 | 0.3927 | 103.40 | 72.60 |
| | 1.7912 | 0.6188 | 116.54 | 65.45 |

[a]Three repeating adsorption operations were done to evaluate these results.

Table 4. Adsorption Capacity of SCD-MgAl-LDH for HQ, DMP, and TBP at Different Concentrations[a]

| | concentration, $c$ (mg/mL) | | | |
|---|---|---|---|---|
| | before adsorption, $C_0$ | after adsorption, $C_e$ | adsorption capacity, $q_e$ (mg/g) | adsorption rate, $\omega$ (%) |
| HQ | 0.4 | 0.0063 | 39.29 | 98.43 |
| | 0.8 | 0.3308 | 46.83 | 58.65 |
| | 1.2 | 0.6559 | 54.41 | 45.34 |
| | 1.6 | 0.9958 | 60.18 | 37.76 |
| | 2.0 | 1.3740 | 62.35 | 31.30 |
| DMP | 0.4 | 0.0191 | 38.02 | 95.23 |
| | 0.8 | 0.0394 | 75.91 | 95.08 |
| | 1.2 | 0.0629 | 113.44 | 94.76 |
| | 1.6 | 0.0856 | 151.44 | 94.65 |
| | 2.0 | 0.1080 | 188.07 | 94.60 |
| TBP | 0.3582 | 0.0195 | 33.80 | 94.56 |
| | 0.7165 | 0.1245 | 59.08 | 82.62 |
| | 1.0747 | 0.2280 | 84.68 | 78.78 |
| | 1.4330 | 0.3669 | 105.97 | 74.40 |
| | 1.7912 | 0.5891 | 119.49 | 67.11 |

[a]Three repeating adsorption operations were done to evaluate these results.

for DMP ($C_0$ = 0.4 mg/mL), and 95% for TBP ($C_0$ = 0.36 mg/mL). Generally, as shown in Tables 3 and 4, both composites illustrated close and preferential adsorptive efficiency for DMP under a much broad concentration range of 0.1−2.0 mg/mL, and for HQ and TBP, the SCD-MgAl-LDH revealed better adsorption compared with SCD-ZnAl-LDH.

The selective adsorption of phenol molecules onto the SCD-LDH composites could be attributed to the different inclusion interaction within the grafted SCD cavities and the adsorption on the exterior of the crystallites. DMP molecule has two methyl groups and one hydroxyl group dispersing on the benzene ring, TBP has one bulky butyl group and one hydroxyl locating on the opposite position, and HQ has only two hydroxyl groups but no alkyl groups. Thus, DMP might have optimal affinity to the SCD-LDH composite due to its compatible hydrophobicity and steric hindrance, compared with TBP with bigger steric hindrance and HQ with low hydrophobicity. So the present two composites gave high selectivity or inclusion ability for DMP in comparison with the other two phenols.

**Characterization for the Solid Samples after Adsorption.** After SCD-ZnAl-LDH adsorbed HQ, BMP and TBP, the XRD patterns (Figure 5) of the solid samples indicated an

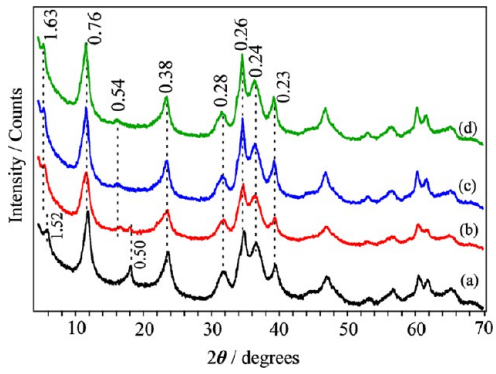


Figure 5. XRD patterns of (a) SCD-ZnAl-LDH and those after SCD-ZnAl-LDH adsorbed (b) HQ, (c) BMPand, (d) TBP, respectively. The $d$-values are given in nanometers.

increase of $d_{basal}$ from 1.51 to 1.62 nm (calculate from ($d_{003}$ + $2d_{006}$ + $3d_{009}$)/3), further verified the entrance of the phenol guests. Similar results were found in CMCD-ZnAl-LDH system,[18,31] for which the inclusion of dodecylbenzene and 5-fluorouracil led to the increase of the interlayer spacing, as shown in Table S1 in the Supporting Information. However, SCD-MgAl-LDH (Figure 6) did not give any change of the $d_{basal}$ (1.61 nm), which may be due to the bigger gallery space


dx.doi.org/10.1021/ic402494m | Inorg. Chem. 2014, 53, 1521−1529

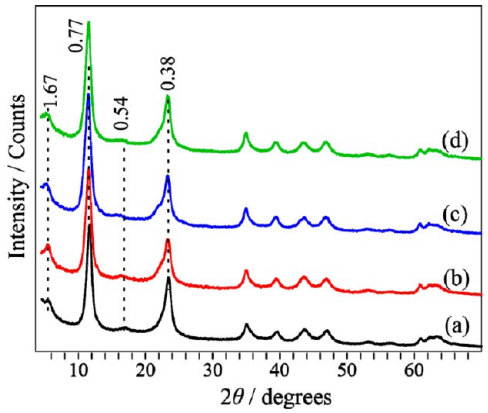


**Figure 6.** XRD patterns for sample of (a) SCD-MgAl-LDH and those after SCD-MgAl-LDH adsorbed (b) HQ, (c) BMP, and (d) TBP, respectively. The *d*-values are given in nanometers.

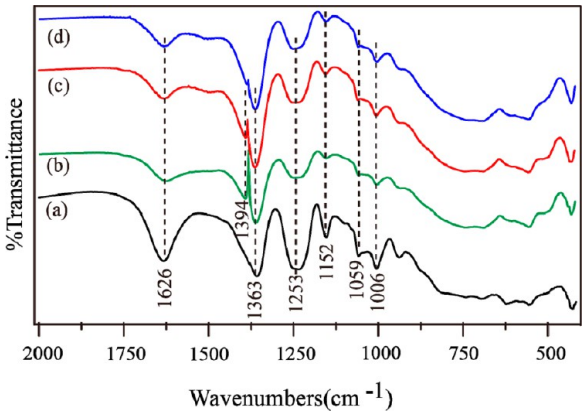


**Figure 7.** FT-IR spectra for (a) SCD-ZnAl-LDH and those after SCD-ZnAl-LDH adsorbed (b) HQ, (c) BMP, and (d) TBP, respectively.

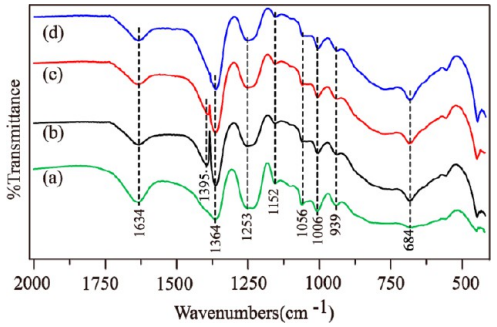


**Figure 8.** FT-IR spectra for (a) SCD-MgAl-LDH and those after SCD-MgAl-LDH adsorbed (b) HQ, (c) BMP, and (d) TBP, respectively.

for the accommodation of the guest. Similar results were observed in some CMCD-ZnAl-LDH[11] and nearly all CMCD-MgAl-LDHs,[14−17] for which the inclusion of bulky guest molecules did not lead to the change of interlayer spacing. The fact that the CD nanocages did not give significant change after introduction of guest species suggests that they may be rigid containers for the inclusion of the guests. Change or not for the $d_{basal}$ after the inclusion of guests may depend on the characteristics of the entered guests, especially the hydrophilic/hydrophobic property or space hindrance. Wei and coworkers[18] proposed the CD intercalated LDHs can be seen as nanocavities with controllable nanocage structure, and they presented swelling/contraction properties in solvents. When the CD nanocage intercalates into the interlayer of LDH, both openings of the CD are blocked by LDH sheets, forming a lockable nanocage. Furthermore, the opening and closing of the nanocages can be controlled based on the swelling property of LDH. When the CD-LDH composite is dispersed in certain solvents, the interlayer spacing expands to give sufficient space for guests to diffuse from solution into the nanocavity of CD. After the solvent is removed by drying, the interlayer spacing decreases to its original size, and the guest is thus retained in the nanocavity. The expansion and contraction of the $d_{basal}$ lead to the opening and closing of the nanocage. Vance and coworkers also found that upon wetting, the $d_{basal}$ of CMCD-MgAl-LDH expanded from 2.06 nm up to 2.68 nm, with an increase of 0.62 nm.[12b] Besides, the FT-IR spectra of the intercalated SCD showed a vibration adsorption band of C−O of phenols at 1394/1395 $cm^{-1}$ after adsorption (Figures 7 and 8), possibly due to the presence of phenolic compounds.

Therefore, this work provides the understanding of molecular recognition ability of the SCD-LDH composites toward the phenol compounds, which demonstrates a potential application in the field of selective separation of these pollutants in wastewater. This kind of composites with nanocage structures can become promising materials because of the synergy of space-confinement of the parent host and supermolecular recognition of the intercalated secondary host.

## CONCLUSIONS

Through calcination−rehydration reactions, the sodium salt of decasulfonated *β*-cyclodextrin [represented as SCD(10)] was reacted with the calcined products (LDO) of ZnAl- and MgAl-$CO_3$-LDHs to form composites with a nanocage structure. The structures and compositions of the composites were fully investigated by XRD, IR, TG-DTA, and elemental analysis. Two nanocomposites showed different basal spacing but similar monolayer SCD orientation being vertical to the LDH layers. Detailed analyses and comparison of the as-prepared SCD-LDH composites and the known carboxymethyl-*β*-cyclodextrin (CMCD) intercalated LDHs have been done. After the combination with the LDH layers, SCD revealed remarkably enhanced thermal stability, with the decomposition temperature heightened by 230 °C. The monolayer arrangement of SCD in the interlayer did not affect the adsorption efficiency, which verified the swelling behavior of the layered compounds in solvent, and the little changed basal spacing after adsorption showed the swelling/constriction properties. Among the three phenol compounds of hydroquinone (HQ), 2,3-dimethylphenol (DMP) and tert-butyl-phenol (TBP) with different hydroxyl and alkyl groups, the two composites showed better selective adsorption for DMP, possibly due to its compatible hydrophobicity and appropriate steric hindrance. For all of the phenolic compounds especially HQ and TBP, SCD-MgAl-LDH gave higher adsorption capacity than SCD-ZnAl-LDH did, showing the difference of the two LDH layers. The synergy of the space-confinement effect of the hydrophilic LDH layer (parent host) and hydrophobic nanocage of the interlayer SCD (secondary host) led to the high selectivity toward the phenol compounds. These SCD-LDH hybrid materials may become potential adsorbents in selective separation of aromatic pollutants in wastewater.


dx.doi.org/10.1021/ic402494m | Inorg. Chem. 2014, 53, 1521−1529

## ■ ASSOCIATED CONTENT

### Supporting Information

The curves of standard aqueous solutions of HQ, DMP, and TBP, CD-LDH intercalates and related inclusion properties. This material is available free of charge via the Internet at http://pubs.acs.org.

## ■ AUTHOR INFORMATION


### Corresponding Author

*E-mail: mashulan@bnu.edu.cn. Fax: +86-10-5880-2075. Telephone: +86-10-5880-7524.


### Notes

The authors declare no competing financial interest.

## ■ ACKNOWLEDGMENTS

This work is supported by the National Science Foundations of China 21271028, 51272030, 21271001, and 21101142.

## ■ REFERENCES


(1) Alberti, G.; Bein, T. *Comprehensive Supramolecular Chemistry*; Pergamon: Oxford, U.K., 1996; p 7. (b) Ogawa, M.; Kuroda, K. *Chem. Rev.* **1995**, *95*, 399. (c) Innocenzi, P.; Brusatin, G. *Chem. Mater.* **2001**, *13*, 3126. (d) Zhu, H. Y.; Lu, G. Q. *Langmuir* **2001**, *17*, 588.

(2) Whittingham, M. S.; Jacobson, A. J., Eds. *Intercalation Chemistry*; Academic Press: New York, 1982.

(3) (a) Constantino, V. R. L.; Pinnavaia, T. J. *Catal. Lett.* **1994**, *23*, 361. (b) Corma, A.; Fornes, V.; Rey, F.; Cervilla, A.; Llopis, E.; Ribera, A. *J. Catal.* **1995**, *152*, 237.

(4) (a) Meyn, M.; Beneke, K.; Lagaly, G. *Inorg. Chem.* **1990**, *29*, 5201. (b) Cavani, F.; Trifiro, F.; Vaccari, A. *Catal. Today* **1991**, *11*, 173.

(5) Fogg, A. M.; Williams, G. R.; Chester, R.; O'Hare, D. *J. Mater. Chem.* **2004**, *14*, 2369.

(6) Darder, M.; López-Blanco, M.; Aranda, P.; Leroux, F.; Ruiz-Hitzky, E. *Chem. Mater.* **2005**, *17*, 1969.

(7) (a) Lv, L.; He, J.; Wei, M.; Duan, X. *Ind. Eng. Chem. Res.* **2006**, *45*, 8623. (b) Fogg, A. M.; Green, V. M.; Harvey, H. G.; O'Hare, D. *Adv. Mater.* **1999**, *11*, 1466. (c) Fogg, A. M.; Dunn, J. S.; Shyu, S. G.; Cary, D. R.; O'Hare, D. *Chem. Mater.* **1998**, *10*, 351. (d) Zhao, Y. F.; He, S.; Wei, M.; Evans, D. G.; Duan, X. *Chem. Commun.* **2010**, *46*, 3031.

(8) (a) Izatt, R. M.; Christensen, J. J. *Synthesis of Macrocycles: The Design of Selective Complexing Agents*; Wiley-Interscience: New York, 1987. (b) Vögtle, F.; Weber, E. *Host Guest Complex Chemistry Macrocycles*; Springer-Verlag: Berlin, 1985.

(9) (a) Lehn, J. M. *Science* **1985**, *227*, 849. (b) Lindoy, L. F. *The Chemistry of Macrocyclic Ligand Complexes*; Cambridge University Press: Cambridge, U.K., 1989. (c) Zhao, H.; Vance, G. F. *Dalton Trans.* **1997**, 1961.

(10) (a) Szejtli, J. *Cyclodextrins and Their Inclusion Complexes*, Akademiai Kiado, Budapest, 1982. (b) Szejtli, J. *J. Inclusion Phenom. Mol. Recognit. Chem.* **1992**, *14*, 25. (c) Bender, M. L.; Komiyama, M. *Cyclodextrin Chemistry*; Springer: Berlin, 1978.

(11) Lan, J.; He, D.; Wei, M. *Chem. Eng. Technol.* **2011**, *34*, 1559.

(12) (a) Wang, J.; Wei, M.; Rao, G.; Evans, D. G.; Duan, X. *J. Solid State Chem.* **2004**, *177*, 366. (b) Zhao, H.; Vance, G. F. *J. Inclusion Phenom.* **1998**, *31*, 305. (c) Sasaki, S.; Yokohama, Y.; Aisawa, S.; Hirahara, H.; Narita, E. *Chem. Lett.* **2005**, *34*, 1192.

(13) (a) Hu, L. F.; Gao, W.; He, J.; Liu, H.; Li, B.; Zhang, X. M. *J. Mol. Struct.* **2013**, *1041*, 151. (b) Liu, X. L.; Meng, L. L. *Korean J. Chem. Eng.* **2013**, *30*, 918. (c) Mohanambe, L.; Vasudevan, S. *Langmuir* **2005**, *21*, 10735. (d) Liu, X. L.; Wei, M.; Li, F.; Duan, X. *AIChE J.* **2007**, *53*, 1591.

(14) Mohanambe, L.; Vasudevan, S. *Inorg. Chem.* **2004**, *43*, 6421.

(15) Mohanambe, L.; Vasudevan, S. *J. Phys. Chem. B* **2005**, *109*, 22523.

(16) Mohanambe, L.; Vasudevan, S. *J. Phys. Chem. B* **2005**, *109*, 11865.

(17) Mohanambe, L.; Vasudevan, S. *Inorg. Chem.* **2005**, *44*, 2128.

(18) Liu, X. L.; Wei, M.; Wang, Z. L.; Evans, D. G.; Duan, X. *J. Phys. Chem. C* **2008**, *112*, 17517.

(19) Jin, L.; Ni, X.; Liu, X.; Wei, M. *Chem. Eng. Technol.* **2010**, *33*, 82.

(20) Tait, R. J.; Thompson, D. O.; Stella, V. J.; Stobaugh, J. F. *Anal. Chem.* **1994**, *66*, 4013.

(21) (a) Chen, F. A.; Evangelista, R. A. *J. Chin. Chem. Soc.* **1999**, *46*, 847. (b) Perrin, C.; Heyden, Y. V.; Maftouh, M.; Massart, D. L. *Electrophoresis* **2001**, *22*, 3203.

(22) Constantino, V. R. L.; Pinnavaia, T. J. *Inorg. Chem.* **1995**, *34*, 883.

(23) Banat, F. A.; Al-Bailey, B.; Al-Asheh, S.; Hayajneh, O. *Environ. Pollut.* **2000**, *107*, 391.

(24) *U.S. EPA Ambient Water Quality Criteria Reports*; Office of Water Regulations and Standards, U.S. Environmental Protection Agency: Washington, D.C., 1980.

(25) Roostaei, N.; Tezel, F. H. *J. Environ. Manage.* **2004**, *70*, 157.

(26) Gonzalez-Serrano, E.; Cordero, T.; Rodriguez-Mirasol, J.; Cotoruelo, L.; Rodriguez, J. J. *Water Res.* **2004**, *38*, 3043.

(27) Zhu, Y. F.; Zhang, L. X.; Schappacher, F. M.; Pöttgen, R.; Shi, J. L.; Kaskel, S. F. *J. Phys. Chem. C* **2008**, *112*, 8623.

(28) Ruan, Z. Q.; You, J. M.; Li, J. B. *Chin. J. Chromatogr.* **2000**, *18*, 184.

(29) Okamoto, K.; Iyi, N.; Sasaki, T. *Appl. Clay Sci.* **2007**, *37*, 23.

(30) He, H. M.; Kang, H. L.; Ma, S. L.; Bai, Y. X.; Yang, X. J. *J. Colloid Interface Sci.* **2010**, *343*, 225.

(31) Jin, L.; Liu, Q.; Sun, Z. Y.; Ni, X. Y.; Wei, M. *Ind. Eng. Chem. Res.* **2010**, *49*, 11176.

(32) Miyata, S. *Clays Clay Miner.* **1975**, *23*, 369.

(33) (a) Iyi, N.; Kurashima, K.; Fujita, T. *Chem. Mater.* **2002**, *14*, 583. (b) Costantino, U.; Coletti, N.; Nocchetti, M.; Aloisi, G. G.; Elisei, F. *Langmuir* **1999**, *15*, 4454.

(34) (a) Huang, G. L.; Ma, S. L.; Zhao, X. H.; Yang, X. J.; Ooi, K. *Chem. Mater.* **2010**, *22*, 1870. (b) Ma, S. L.; Du, L.; Wang, J.; Chu, N. K.; Sun, Y. H.; Sun, G. B.; Yang, X. J.; Ooi, K. *Dalton Trans.* **2011**, *40*, 9835.

(35) Bratu, I.; Astilean, S.; Ionesc, C.; Indrea, E.; Huvenne, J. P.; Legrand, P. *Spectrochim. Acta A: Mol. Biomol. Spectrosc.* **1998**, *54*, 191.

(36) Kolics, A.; Polkinghorne, J. C.; Wieckowski, A. *Electrochim. Acta* **1998**, *43*, 2605.

(37) (a) Douhal, A. *Chem. Rev.* **2004**, *104*, 1955. (b) Sanchez, A. M.; de Rossi, R. H. *J. Org. Chem.* **1996**, *61*, 3446.